Kinetic Differences in the Chlorination of Cephalosporin versus Carbacephalosporin Enols: Evidence of Sulfur Neighboring Group Participation

John E. Burks, Jr.,* Erik C. Chelius,* and Ross A. Johnson

Lilly Research Laboratories, Eli Lilly and Company, Lafayette, Indiana 47902

Received February 14, 1994®

Intermediates in the chlorination of carbacephalosporin and cephalosporin enols with chlorotriphenoxyphosphonium chloride, $(PhO)_3P^+Cl\ Cl^-$, have been characterized at low temperatures by NMR. ^{31}P NMR has been used to determine the rate constants and Arrhenius activation energies for the chlorination of the cephalosporin enol **1b** and the carbacephalosporin enol **1c**. The results show a 3.7 kcal/mol lower activation energy for the chlorination of the cephalosporin enol. Semiempirical and ab initio calculations have been employed to evaluate chloride attack and phosphate departure for model cephalosporin and carbacephalosporin enols. The experimental and computational results are consistent with a chlorination mechanism that involves rapid, reversible chloride addition to an intermediate enol phosphonium species followed by rate-limiting phosphate departure. The lower activation energy for phosphate departure in the cephalosporin case is attributed to sulfur neighboring group participation.

Introduction

As a part of our overall effort to manufacture the carbacephalosporin antibiotic LY163892,[1] we required the conversion of 3-hydroxy-1-carba-3-cephem **1a** to 3-chloro-1-carba-3-cephem **2a** (eq 1). Our approach was

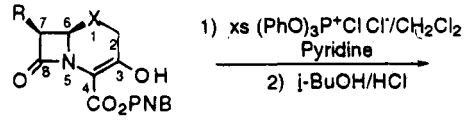

1a: X = CH_2, R = $NHCOCH_2OPh$
1b: X = S, R = $NHCOCH_2OPh$

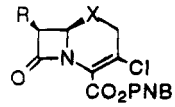

(1)

2a: X = CH_2, R = NH_2 HCl
2b: X = S, R = NH_2 HCl

based upon well-established chemistry for the transformation of 3-hydroxy-3-cephem **1b** to 3-chloro-3-cephem **2b**.[2] Early in the course of our work it became apparent that **1a** exhibits a significantly slower conversion under the same conditions as employed for the chlorination of **1b**. Whereas **1b** undergoes chlorination in high yield (ca. 85%) within 60 min at temperatures below −10 °C,[2] **1a** requires temperatures of greater than 20 °C for several hours to obtain modest yields (ca. 50%) of the desired chlorination product.

Since the two substrates differ in the replacement of a sulfur by a methylene group in the β-position relative to the reaction site, the potential for neighboring group participation was considered as a possible explanation for the reactivity difference. The participation of sulfur in the interconversion of cephams and penams via an episulfonium intermediate has been recognized for some time;[3] however, we have not isolated or detected any products during the chlorination of **1b** that would clearly implicate the formation of an episulfonium intermediate during the course of this reaction. In a study of neighboring group participation by sulfur in the solvolytic interconversion between penam and cepham systems, Tsushima and Tanida[4] reported that the 3β-chloro-3α-methylcepham **3** shows no influence of the neighboring

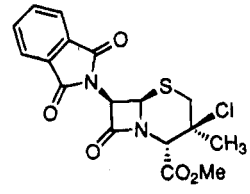

3

β-sulfur on its rate of solvolysis when compared with some simple model substrates. The model substrates, however, did not include an actual carbacephalosporin.

The marked difference in the reactivity observed for **1a** and **1b** has led us to a more careful examination of this chlorination reaction. Furthermore, our interest in the synthesis of carbacephalosporins has afforded us better substrates for examining differences in reactivity between these two molecular frameworks. Because the carbacephalosporins are a relatively new class of compounds and their chemistry has not been extensively explored, a better understanding of the factors that distinguish this class of compounds from the cephalosporins is of interest.

® Abstract published in *Advance ACS Abstracts,* August 15, 1994.

(1) Bodurow, C. C.; Boyer, B. D.; Brennan, J.; Bunnell, C. A.; Burks, J. E.; Carr, M. A.; Doecke, C. W.; Eckrich, T. M.; Fisher, J. W.; Gardner, J. P.; Graves, B. J.; Hines, P.; Hoying, R. C.; Jackson, B. G.; Kinnick, M. D.; Kochert, C. D.; Lewis, J. S.; Luke, W. D.; Moore, L. L.; Morin, J. M., Jr.; Nist, R. L.; Prather, D. E.; Sparks, D. L.; Vladuchick, W. C. *Tetrahedron Lett.* **1989**, *30*, 2321–2324.

(2) Hatfield, L. D.; Blaszczak, L. C.; Fisher, J. W. U.S. Patent 4,226,986, 1980.

(3) (a) Kukolja, S.; Lammert, S. R. *J. Am. Chem. Soc.* **1972**, *94*, 7169–7170. (b) Kukolja, S.; Lammert, S. R.; Gleissner, M. R.; Ellis, A. I. *J. Am. Chem. Soc.* **1975**, *97*, 3192–3198. (c) Balsamo, A.; Giorgi, I.; Macchia, B.; Macchia, F.; Rosai, A.; Domiano, P.; Nannini, G. *J. Org. Chem.* **1980**, *45*, 2610–2614. (d) Balsamo, A.; Macchia, B.; Macchia, F.; Rossello, A.; Scatena, P.; Domiano, P. *J. Org. Chem.* **1986**, *51*, 540–543. (e) Balsamo, A.; Benvenuti, M.; Lapucci, A.; Macchia, B.; Nencetti, S.; Rossello, A.; Macchia, R.; Domiano, P.; Dradi, E. *J. Org. Chem.* **1991**, *56*, 2148–2153.

(4) Tsushima, T.; Tanida, J. *J. Org. Chem.* **1980**, *45*, 3205–3211.

0022-3263/94/1959-5724$04.50/0

Scheme 1

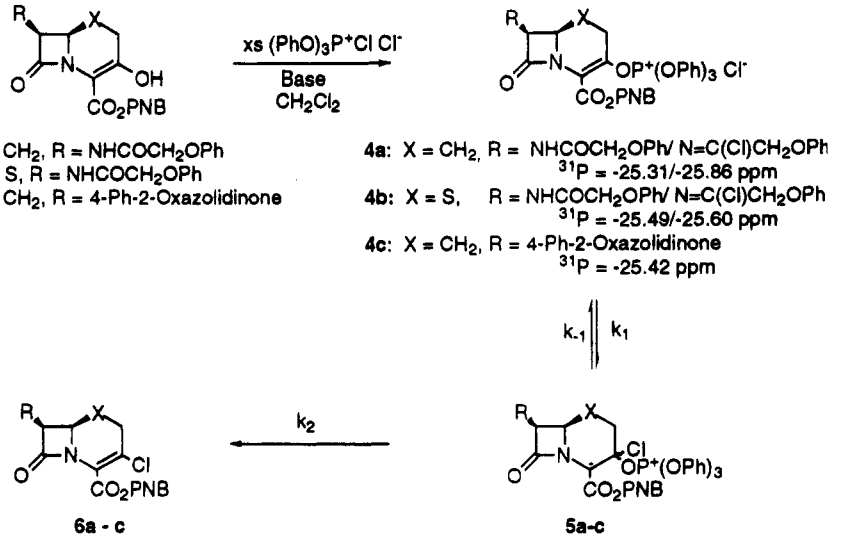

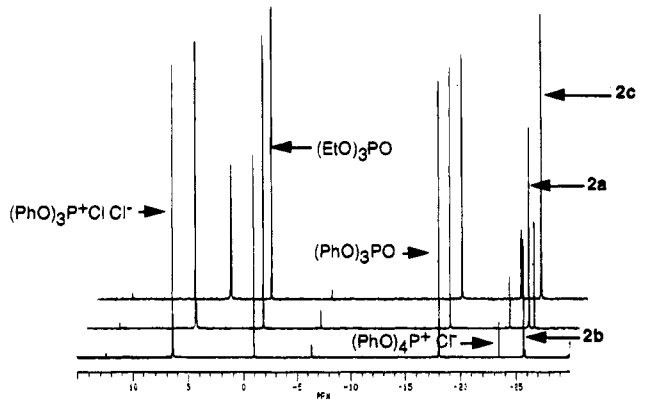

Figure 1. Typical ^{31}P NMR spectra for the reactions of enols **1a–c** with $(PhO)_3P^+Cl\ Cl^-$. The spectra are stacked and offset so that the scale is relevant only to the first spectrum.

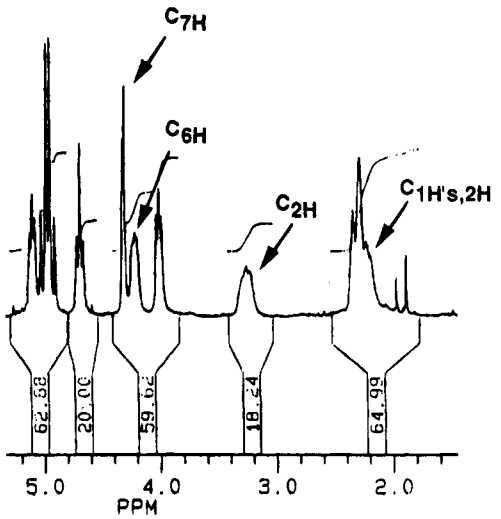

Figure 2. ^1H NMR spectral region that contains the protons on the carbacephalosporin and oxazolidinone ring for **4c**.

We report herein results of a comparative study of the kinetics of the chlorinations of carbacephalosporin and cephalosporin enols together with results for transition state calculations for the chlorination of model carbacephalosporin and cephalosporin enols. These results provide a clear indication of sulfur neighboring group participation for reactions in which positive charge develops at C-3 in the cephalosporin ring system.

Results and Discussion

Scheme 1 outlines a simplified reaction pathway for the conversion of enols **1a–c** to the corresponding chlorides by the action of the chlorination reagent formed upon combination of triphenyl phosphite with chlorine $[(PhO)_3P^+Cl\ Cl^-]$.[5] As shown in Figure 1, ^{31}P NMR analyses of reaction solutions obtained immediately upon mixing enols **1a–c** with CH_2Cl_2 solutions of the chlorination reagent show in each case one or two new signals between −25 and −26 ppm, in addition to signals assigned to $(PhO)_3P^+Cl\ Cl^-$, triphenyl phosphate, and $(PhO)_4P^+Cl^-$.[6] In the case of enol **1c**, a single major new phosphorus signal is observed at −25.42 ppm to which we have assigned structure **4c**.[7] This assignment is based upon ^1H and ^{13}C NMR analyses at −20 °C of reaction mixtures obtained upon titration of enol **1c** with a CD_2Cl_2 solution of $(PhO)_3P^+Cl\ Cl^-$. The ^1H NMR spectral region that contains the protons attached to the carbacephalosporin and oxazolidinone rings of **4c** is shown in Figure 2. Assignments were facilitated by 2D NMR COSY and HETCOR experiments. Further support for the assignment of **4c** as the structure of the reaction intermediate versus a protonated form of **5c** comes from the identification of C-3 (147.12 ppm, d, $^2J_{PC}$ = 13.1 Hz) through observation of long-range C—H coupling between this carbon and the C-2 protons. The chemical shift clearly supports the sp^2 hybridization of this carbon.

We indicate a tetracoordinate phosphorus cation in structure **4c** with an associated chloride anion. The phosphorus signal for **4c** is observed in a region where signals assigned to both tetracoordinate phosphonium

(5) (a) Tseng, C. K. *J. Org. Chem.* **1979**, *44*, 2793–2794. (b) Michalski, J.; Pakulski, M.; Skowronska, A. *J. Org. Chem.* **1980**, *45*, 3122–3123.

(6) The $(PhO)_4P^+\ Cl^-$ arises from the reaction of phenol that is present in the triphenyl phosphite with the chlorination reagent. The chemical shift for $(PhO)_4P^+\ Cl^-$ is reported as −22.8 ppm in CH_2Cl_2, which is very similar to that for the phosphorus intermediates observed in this reaction. Dennis, L. W.; Bartuska, V. J.; Maciel, G. E. *J. Am. Chem. Soc.* **1982**, *104*, 230–235.

(7) Enol **1c** was chosen as the substrate for characterization of the phosphorus intermediate in this reaction because it afforded a phosphorus species that was stable for days at temperatures below −30 °C, and the 4-phenyl-2-oxazolidinone group was not subject to reaction with the chlorination reagent.

Table 1. k_{obs} for the Chlorination of Enols 1b and 1c[a]

temp (°C)	enol **1b** k_{obs} (s^{-1})	temp (°C)	enol **1c** k_{obs} (s^{-1})
−41.7	8.37 (10^{-6})	−3.2	2.38 (10^{-6})
−36.2	2.20 ± 0.22 (10^{-5})	9.9	2.66 ± 0.01 (10^{-5})
−25.2	1.81 ± 0.16 (10^{-4})	16.5	7.23 ± 0.89 (10^{-5})
		24.2	2.20 ± 0.15 (10^{-4})
25.0	3.45 (10^{-1})[b]	25.0	2.42 (10^{-4})[b]

[a] k_{obs} values are the average of three replicates except for the lowest temperature run in each series in which case only a single run was conducted. [b] Calculated rate constant.

species and pentacoordinate phosphoranes have been reported.[6] The only chemical evidence we offer in support of the tetracoordinate phosphonium structure rather than a pentacoordinate phosphorane structure with chlorine as a ligand is the failure to observe any change in the phosphorus chemical shift for **4c** upon the addition of an excess of $SbCl_5$.[5b]

By analogy the intermediates formed upon reaction of enols **1a** and **1b** with excess $(PhO)_3P^+Cl\ Cl^-$ are assigned to structures **4a** and **4b**. The fact that two signals are observed in these cases is due to competing reaction of the secondary phenoxyacetamido group to form the corresponding imidoyl chloride.[8] The lower field signal in each case is assigned to the enol phosphonium species **4a** and **4b** in which the phenoxyacetamido group remains intact. The higher field signal is assigned to the enol phosphonium species in which the phenoxyacetamido group has been converted into the corresponding imidoyl chloride by the action of excess $(PhO)_3P^+Cl\ Cl^-$. Conversion of the amide to the imidoyl chloride is monitored through disappearance of the amide NH resonance in the ^1H NMR spectrum of the reaction mixture. Changes in the phosphorus signals are coincident with the disappearance of the NH resonance.[9]

The rates of chlorination of enols **1b** and **1c** were determined by monitoring the disappearance of the intermediates **4b** and **4c** over time by ^{31}P NMR. Confirmation of enol chlorination was secured by HPLC analysis of the final reaction mixture following quenching into aqueous acetonitrile to afford the 3-chloro derivatives **7a−c** (eq 2).[10] Plots of the natural log of the area of the

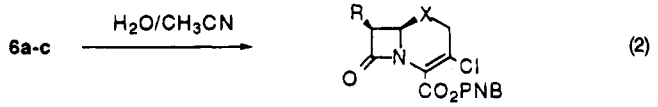

(2)

7a: X = CH_2, R = $NHCOCH_2OPh$
7b: X = S, R = $NHCOCH_2OPh$
7c: X = CH_2, R = 4-Ph-2-Oxazolidinone

phosphorus intermediate signal versus time show good linear correlations ($R^2 > 0.99$). The results for kinetic runs over a range of temperatures are shown in Table 1. Arrhenius plots of ln k_{obs} versus $1/T$ for both sets of data afford linear correlations ($R^2 > 0.99$) and give activation energies of 22.0 and 25.7 kcal/mol for the chlorination of **1b** and **1c**, respectively.

The above results clearly show a dramatic difference between the rates of chlorination of the enols **1b** and **1c**. Extrapolated rate constants for **1b** and **1c** at 25 °C are $3.45 \times 10^{-1}\ s^{-1}$ and $2.42 \times 10^{-4}\ s^{-1}$, respectively, which represents *at least a 10^3 rate difference*. That this difference is not due to the nature of the amide at C-7 has been shown by evaluation of the rate of chlorination of **1a** at −3 °C. Although this analysis is complicated by competing chlorination of the phenoxyacetamido group,[11] the rate constant could be estimated by fitting the ^{31}P NMR data to a kinetic model which included rate constants to account for the competing phenoxyacetamide chlorination.[12] An upper limit of $1.7 \times 10^{-5}\ s^{-1}$ was derived for the enol chlorination of **1a** compared with $k_{calcd} = 7.3 \times 10^{-3}\ s^{-1}$ for the chlorination rate constant of enol **1b** at −3 °C. Thus, at least a *440-fold rate acceleration* is attributable to the presence of the sulfur β to the reaction center.

The transannular participation of sulfur in solvolysis reactions is well recognized;[13] and as noted earlier, the interconversion of cepham and penam systems has been taken as evidence for the formation of a common episulfonium ion within these bicyclic frameworks. Although the reaction under study here is an addition−elimination process and not a solvolysis reaction, it bears similarity in that as the phosphate departs there will be buildup of positive charge at C_3. In the case of the cephalosporin this charge will be β to sulfur.

In order to evaluate the ability of sulfur to stabilize a β-positive charge with respect to carbon, the energies of a series of isodesmic reactions were calculated (eqs 3−5).[14] The results of these calculations are listed in

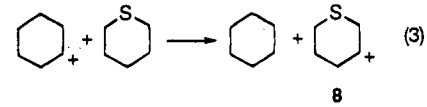

(3)

8

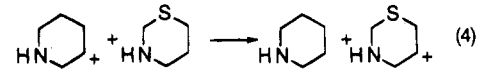

(4)

9

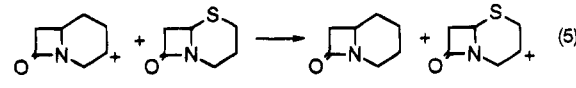

(5)

10

Table 2. All of the energies of reaction are negative at the levels of theory investigated. The S−C_2 and S−C_3 distances in the optimized sulfur containing cations (**8**−**10**) are nearly the same, which is consistent with the formation of an episulfonium ion and in agreement with the rationale for the enhanced rate of solvolysis of

(8) (a) Hatfield, L. D.; Lun, W. H. W.; Jackson, B. G.; Peters, L. R.; Blaszczak, L. C.; Fisher, J. W.; Gardner, J. P.; Dunigan, J. M. In *Recent Advances in the Chemistry of β-Lactam Antibiotics*; Gregory, G. I., Ed.; The Royal Society of Chemistry: Burlington House, London, 1980; pp 109−124. (b) Hatfield, L. D.; Blaszczak, L. C.; Fisher, J. W. U.S. Patent 4,211,702, 1980.

(9) We have not observed any ^{31}P NMR signal during the course of the chlorinations of enols **1a−c** that could be attributed to a phosphorus intermediate in the conversion of the amide to the imidoyl chloride. Control ^{31}P NMR experiments for the amide chlorination of 3-chloro-7-phenoxyacetamide **7a** showed only a signal for triphenyl phosphate.

(10) The chlorinations of enols **1a** and **1c** are accompanied by the formation of minor amounts of the Δ^2-3-chloro olefinic isomer and some cleavage of the *p*-nitrobenzyl ester protecting group. HPLC analyses, however, confirmed the expected 3-chloro products as the major product for each reaction.

(11) The phenoxyacetamido group of **1b** does not undergo chlorination at a significant rate over the temperature range for which its enol functionality is chlorinated. A small amount of **2b** in which the amide has been chlorinated is observed at the beginning of the kinetic analysis due to amide chlorination caused by sample warming during transfer from the initial reaction vial to the NMR tube.

(12) The ^{31}P NMR data were fit to a kinetic model by using the program SimuSolv. Trademark of The Dow Chemical Corp.

(13) Ikegami, S.; Asai, T.; Tsuneoka, K.; Matsumura, S.; Akaboshi, S. *Tetrahedron* **1974**, *30*, 2087−2092.

(14) All calculations were completed with: (a) MOPAC 5.0 using the PM3 Hamiltonian. Stewart, J. J. P. *J. Comput. Chem.* **1989**, *10*, 221. (b) SPARTAN, Wavefunction, Inc., Irvine, CA 92715. (c) Hehre, W. J.; Radom, L.; Schleyer, P. v. R.; Pople, J. A. *Ab Initio Molecular Orbital Theory*; Wiley: New York, 1986.

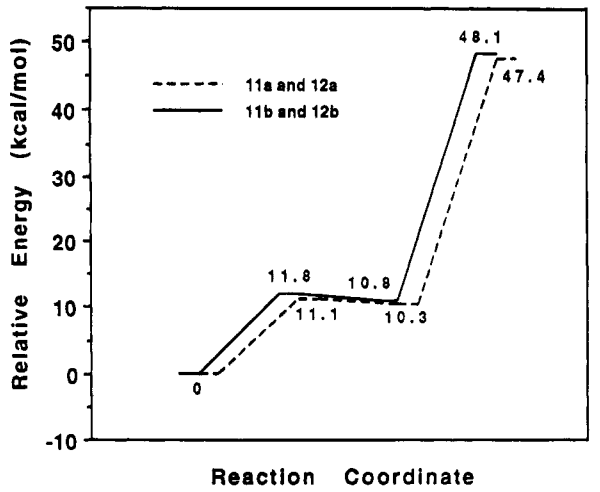

Figure 3. Relative energy of chloride attack and phosphate departure for **11** and **12**, respectively.

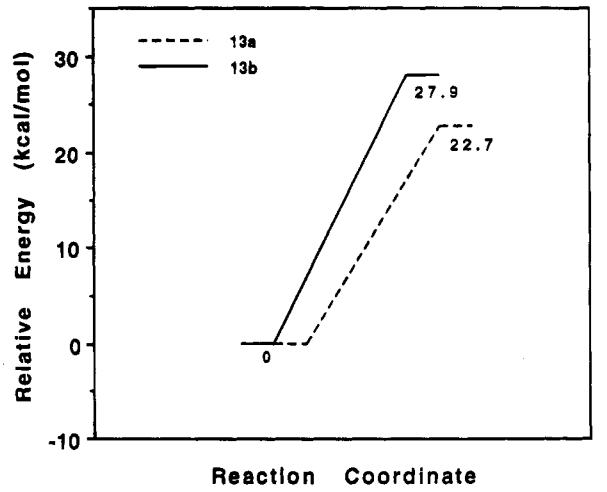

Figure 4. Relative energy of phosphate departure for **13**.

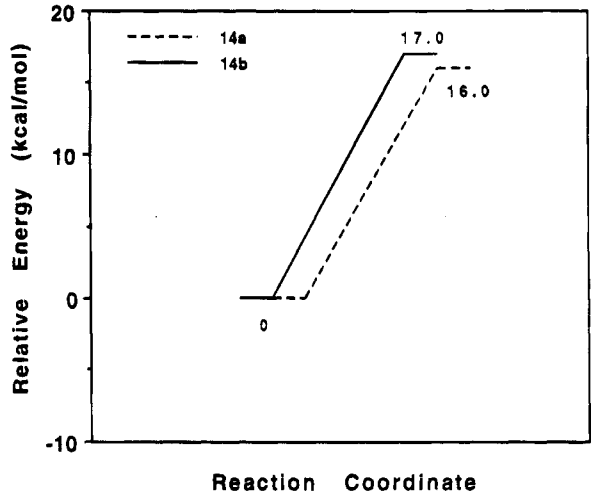

Figure 5. Relative energy of phosphate departure for **14**.

Table 2. Isodesmic Reaction Energies

theory	eq 3 (kcal/mol)	eq 4 (kcal/mol)	eq 5 (kcal/mol)
AM1	−9.6	−8.2	−5.0
PM3	−11.9	−10.6	−8.7
STO-3G//STO-3G	−38.7	−39.9	−39.9
3-21G(*)//3-21G(*)	−13.3	−15.7	−9.5
6-31G*//3-21G(*)	−14.7	−15.9	−12.4

tetrahydro-3-thiopyranol versus cyclohexanol[13] and the proposed pathway for the solvolytic interconversion of 3-chloro- and 3-hydroxycephams to 2-substituted methylpenicillins.[3]

In an effort to gain insight into the relative energies of chloride attack versus phosphate departure, the ground states and transition states for chloride attack and phosphate departure for model systems **11**−**14** were

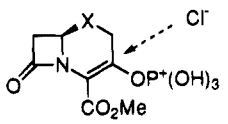

11a: X = S
11b: X = CH_2

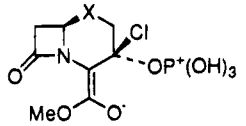

12a: X = S
12b: X = CH_2

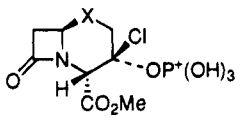

13a: X = S
13b: X = CH_2

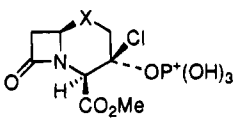

14a: X = S
14b: X = CH_2

located using the PM3 Hamiltonian. Since it is not known if the presumed enolate intermediate is protonated prior to phosphate departure both the nonprotonated (**12**) and protonated (**13**, **14**) intermediates were examined. The calculated heats of formation of the starting ground states and transition states involving β-face chloride attack and α-face phosphate departure are listed in Table 3 and depicted graphically in Figures 3−5. The single imaginary vibrational frequency for chloride attack is consistent with Cl−C_3 bond formation, whereas the single imaginary frequency for phosphate departure corresponds to O−C_3 bond breaking. The less favored α-face chloride attack, which puts the phosphate group in an axial position, and β-face phosphate departure gave similar results.

The relative transition state energies predict that the energy of activation for phosphate departure is 1.5−3 times greater than that for chloride attack.[15] In addition, the relative transition state energies are consistent with the lower energy of activation measured for the cephalosporin versus the carbacephalosporin. These calculations support a mechanism that involves rate-limiting phosphate departure, which is accelerated by the presence of sulfur in the cephalosporin.

Examination of the highest filled molecular orbitals involving sulfur in the model cations **8**−**10** show significant delocalization across C_2 and C_3. Although some delocalization is evident in the transition states involving phosphate departure, particularly in the cases of **13a** and **14a**, it is not nearly as extensive. This delocalization becomes more evident as phosphate departs from transition states **13a** and **14a**. The PM3 Mulliken bond orders (Table 4) confirm the extensive delocalization observed for cations **8**−**10** and indicate that little through-space delocalization is occurring between sulfur and C_3 in the transition states **12**−**14**. These results suggest that a mechanism other than nonvertical participation is responsible for the observed 440-fold rate acceleration.

(15) Stewart, J. J. P. In *Reviews in Computational Chemistry*; Lipkowitz, K. B., Boyd, D. B., Eds.; VCH: New York, 1990; pp 68−69.

Table 3. Ground State Starting and Transition State Heats of Formation

	X = S (**11**–**14a**)		X = CH_2 (**11**–**14b**)	
structure	starting (kcal/mol)	transition (kcal/mol)	starting (kcal/mol)	transition (kcal/mol)
11 [Cl^- attack]	−356.9	−345.8	−376.9	−365.1
12 [$(HO)_3PO$ departure]	−346.6	−309.5	−366.1	−328.8
13 [$(HO)_3PO$ departure]	−182.1	−159.4	−210.9	−183.0
14 [$(HO)_3PO$ departure]	−176.9	−160.9	−202.0	−185.0

Table 4. PM3 Mulliken Bond Orders for Cations 8–10 and Transition States 12–14[a]

cation	X–C_2	X–C_3	C_2–C_3
8, X = S	0.93 (1.85)	0.89 (1.88)	1.02 (1.49)
9, X = S	0.93 (1.85)	0.92 (1.87)	1.01 (1.49)
10, X = S	0.93 (1.86)	0.90 (1.89)	1.02 (1.49)
12a, X = S	0.98 (1.82)	0.01 (2.84)	1.00 (1.49)
12b, X = CH_2	0.99 (1.52)	0.00 (2.51)	0.99 (1.50)
13a, X = S	0.95 (1.82)	0.04 (2.73)	1.01 (1.49)
13b, X = CH_2	0.96 (1.53)	0.02 (2.47)	1.00 (1.50)
14a, X = S	0.96 (1.82)	0.03 (2.76)	0.99 (1.50)
14b, X = CH_2	0.97 (1.53)	0.02 (2.48)	0.99 (1.51)

[a] The distances between atoms in angstroms are listed in parentheses.

Conclusions

The reaction of cephalosporin or carbacephalosporin enols with $(PhO)_3P^+Cl\ Cl^-$ affords an intermediate enol phosphonium species as evidenced by low-temperature NMR studies. The carbacephalosporin-derived enol phosphonium species are stable for days at temperatures below −20 °C. We believe that these intermediates are converted to the corresponding vinyl chlorides through a subsequent addition–elimination mechanism that involves reversible chloride addition to the initially formed enol phosphonium intermediate followed by rate-limiting phosphate departure.[16] We see no evidence to suggest the formation of an episulfonium ion in either case. Although we do not know the orientation of the phosphate leaving group in our system, the computational results suggest sulfur participation should facilitate both α- and β-face phosphate departure with α-face departure favored. Our kinetic results clearly indicate a rate acceleration in the chlorination of enol **1b**, which we attribute to the ability of the sulfur to stabilize the developing positive charge at the β-position during phosphate departure. These results represent the first quantitative comparison of rate differences for a key transformation in the synthesis of these biologically important molecules.

Experimental Section

General. Commercial grade solvents were stored over 4-Å molecular sieves for at least 24 h prior to use. Quinoline and triphenyl phosphite were purchased from commercial vendors and used without further purification. ^1H, ^{13}C, and ^{31}P NMR spectra were recorded on a Bruker AC-E 300 spectrometer with a QNP probe at operating frequencies of 300.13, 75.47, and 121.50 MHz, respectively. ^1H and ^{13}C NMR chemical shifts are reported relative to TMS, and ^{31}P NMR chemical shifts are reported relative to 85% H_3PO_4, uncorrected for temperature effects. Variable temperature for NMR experiments was maintained by using a BVT-100 variable-temperature control unit. The probe temperature was calibrated by using the chemical shifts of methanol. Quantitative ^{31}P NMR was performed with standard solutions of triethyl phosphate in acetone-d_6 contained in a Wilmad WGS-5BL coaxial insert.[17] Analytical HPLC was conducted on a 25 cm × 4.6 mm i.d. Zorbax C8 column with 1:1 isocratic eluent system of 0.1 M H_3PO_4 (pH 2.5):CH_3CN at a flow rate of 1.5 mL/min, a column temperature of 25 °C, and UV detection at 220 nm.

General Procedure for the Determination of the Rate Constants for the Chlorination of Enols 1a,[18] 1b,[19] and 1c by NMR. A 2-mL microvial, equipped with a magnetic stir bar and N_2 supply, was charged with 0.12 mmol of enol **1a**, **1b**, or **1c**. The vial was cooled in a dry ice/acetone bath, and 0.6 mL of ~0.7 M $(PhO)_3P^+Cl\ Cl^-$ in CH_2Cl_2 was added via syringe. The mixture was stirred for ~1 min and then transferred to a 5-mm NMR tube which was precooled in a dry ice/acetone bath. A Wilmad WGS-5BL coaxial insert, which contained a 1.01 M reference standard solution of triethyl phosphate in acetone-d_6, was inserted, and the sample was transferred within 3–4 min of mixing to a probe which had been equilibrated at the desired reaction temperature. Data acquisition was begun 15 min after mixing. ^1H-decoupled ^{31}P spectra were acquired as 16 or 32 scans, 64K FID's with a sweep width of 7250 Hz, 1.1 s pulse width (~26°), and a 15 s delay between pulses. Spectra were acquired over at least 3 half-lives except for the chlorination of **1c** at −3 °C, which had proceeded to only ~30% completion after 48 h. Peak areas were referenced to the triethyl phosphate standard and were integrated manually. Linear plots of the natural logarithm of the areas of **4b** and **4c** versus time with correlation coefficients of >0.990 were observed in all cases. Upon completion of the kinetic run, the samples were withdrawn from the probe and transferred to a 100-mL volumetric flask, which contained 10 mL of 1:1 CH_3CN:H_2O. Following sonication, the samples were analyzed by HPLC. In the case of enol **1c**, the 3-chlorination product **7c** was confirmed as the major product by HPLC with *p*-nitrobenzyl chloride and the Δ^2-isomer of **7c** observed as byproducts along with varying amounts of unreacted **1c**. For enols **1a** and **1b**, HPLC analyses confirmed **7a** and **7b** as the major reaction product.

Acknowledgment. The authors would like to thank Mr. Jack Fisher, Mr. Jim Dunnigan, and Mr. Richard Hoying for supplying enol **1c**. We would also like to thank Drs. David Wirth, Fred Perry, and Lowell Hatfield for helpful discussions on the chlorination chemisty and Dr. Don Boyd for advice on the computational work.

Supplementary Material Available: Long-range ^1H–^{13}C shift correlation that shows C-3 coupling to C-2 protons, two representative plots of the kinetic data for the chlorination of **1b** and **1c**, Arrhenius plots for the chlorination of enols **1b** and **1c**, atomic coordinates for the 3-21G(*) optimized structures **8**–**10**, and atomic coordinates for the PM3 transition state structures **11**–**14** (17 pages). This material is contained in libraries on microfiche, immediately follows this article in the microfilm version of the journal, and can be ordered from the ACS; see any current masthead page for ordering information.

(16) The concentration of **5** (Scheme 1) is assumed to be negligible. For this kinetic scheme the disappearance of **4** and the appearance of **6** are described by $k_{obs} = k_1k_2/(k_{-1} + k_2)$. Connors, K. A. *Chemical Kinetics: The Study of Reaction Rates in Solution*; VCH: New York, 1990; pp 100–101.

(17) Stanislawski, D. A.; VanWazer, J. R. *Anal. Chem.* **1980**, *52*, 96.

(18) Jackson, B. G.; Gardner, J. P.; Heath, P. C. *Tetrahedron Lett.* **1990**, *31*, 6317–6320.

(19) Chauvette, R. R.; Pennington, P. A. *J. Med. Chem.* **1975**, *18*, 403–408.